ACS MATERIALS Au
AN OPEN ACCESS JOURNAL OF THE AMERICAN CHEMICAL SOCIETY

pubs.acs.org/materialsau
Article

Photobleaching of Light-Activated Porphyrin-Functionalized Plastic Coupons for Potential Antimicrobial Applications

Grace M.O. Tieman, Fatima Shatila, Stefania Ceschia, Jeremy E. Wulff, and Heather L. Buckley*

Cite This: ACS Mater. Au 2025, 5, 537−546
Read Online

ABSTRACT: Developing greener alternatives for harmful conventional cleaning agents is an important focus for preventing negative impacts on both the environment and human health. One potential alternative of interest is photodynamic inactivation (PDI), where a photosensitizing molecule is used to generate singlet oxygen ($^1O_2$) and other reactive oxygen species (ROS). ROS, $^1O_2$ in particular, are known to react with cellular membranes of bacteria, resulting in cellular death. Porphyrinoids are one of these known light sensitizing species. In this work, zinc(II) 5,10,15,20-tetrakis((*N*-4-[3-(trifluoromethyl)-3*H*-diazirin-3-yl]benzyl)-4-pyridyl)-21*H*,23*H*-porphine tetrabromide is covalently attached to polyethylene terephthalate (PET) via thermal activation of a diazirine to initiate a C−H insertion. With the porphyrin now covalently bonded to the PET, the functionalized PET was assessed at a range of light intensities on its ability to generate $^1O_2$ and for antimicrobial activity against *Escherichia coli*; the results were found to be correlated. Because photobleaching and resultant loss of activity are one of the weaknesses of PDI, the material was further assessed for its ability to withstand various photobleaching conditions. The photobleaching conditions assessed were high intensity light in dry and underwater conditions and ambient light, along with a set of dark controls. Results indicate that after 2 weeks of high intensity irradiation, the material still mediates singlet oxygen generation, albeit less efficiently. This shows promise for the use of this approach as an alternative to conventional cleaning agents.

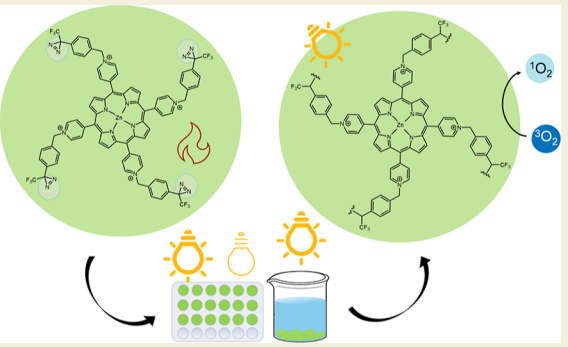

KEYWORDS: *antimicrobial, photodynamic inactivation, porphyrin, diazirine, durability*

1. INTRODUCTION

Bacterial growth on surfaces is becoming more concerning due to the various diseases and infections that bacteria can cause, and as bacterial resistance becomes more prevalent.[1−4] The diseases that can be caused by bacteria include, but are not limited to, blood infections, scarlet fever, tuberculosis, and typhoid fever.[1,3] Bacterial spread on surfaces is particularly serious in hospitals due to the combination of a vulnerable population present and an environment containing additional bacteria present from the people who are infected or ill; this leads to hospital-acquired infections.[1,5−7] Bacterial growth is also a known problem in the food industry in packaging or on food processing surfaces.[7,8] Additionally, the growth of biofilms in water treatment systems negatively impacts human health and the environment, while also increasing costs during the water treatment process.[9,10] Water is typically treated and disinfected in these facilities primarily using chlorine, while other chlorine-based disinfectants (CBDs) are used for disinfection in other settings like in the medical field and households.[11−13]

Chlorine and CBDs typically kill cells through an oxidative mechanism with the cellular membrane. This mechanism of action, combined with overapplication, causes bacterial resistance against these molecules.[4,14] Not only are these halogenated cleaners typically persistent in the environment themselves but they also react with other organic material, found in both drains and the environment, to produce disinfection byproducts (DBPs).[11,13] There have been more than 600 derivatives of DBPs found in aqueous environments, some of which are controlled for and studied whereas others are not.[13,15,16] Additionally, use of CBDs leads to an increase of HCl, HOCl, and chlorine atoms in the environment, which can lead to the formation of NO_x compounds at higher altitudes; NO_x compounds contribute to ozone layer depletion.[11,17] There has been an emphasis on investigating the impact of CBDs in the environment as a result of the increase in disinfection during the COVID-19 pandemic.[11,12,18] Thus, greener alternatives to conventional cleaning agents are

Received: December 11, 2024
Revised: February 19, 2025
Accepted: February 20, 2025
Published: March 4, 2025

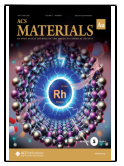

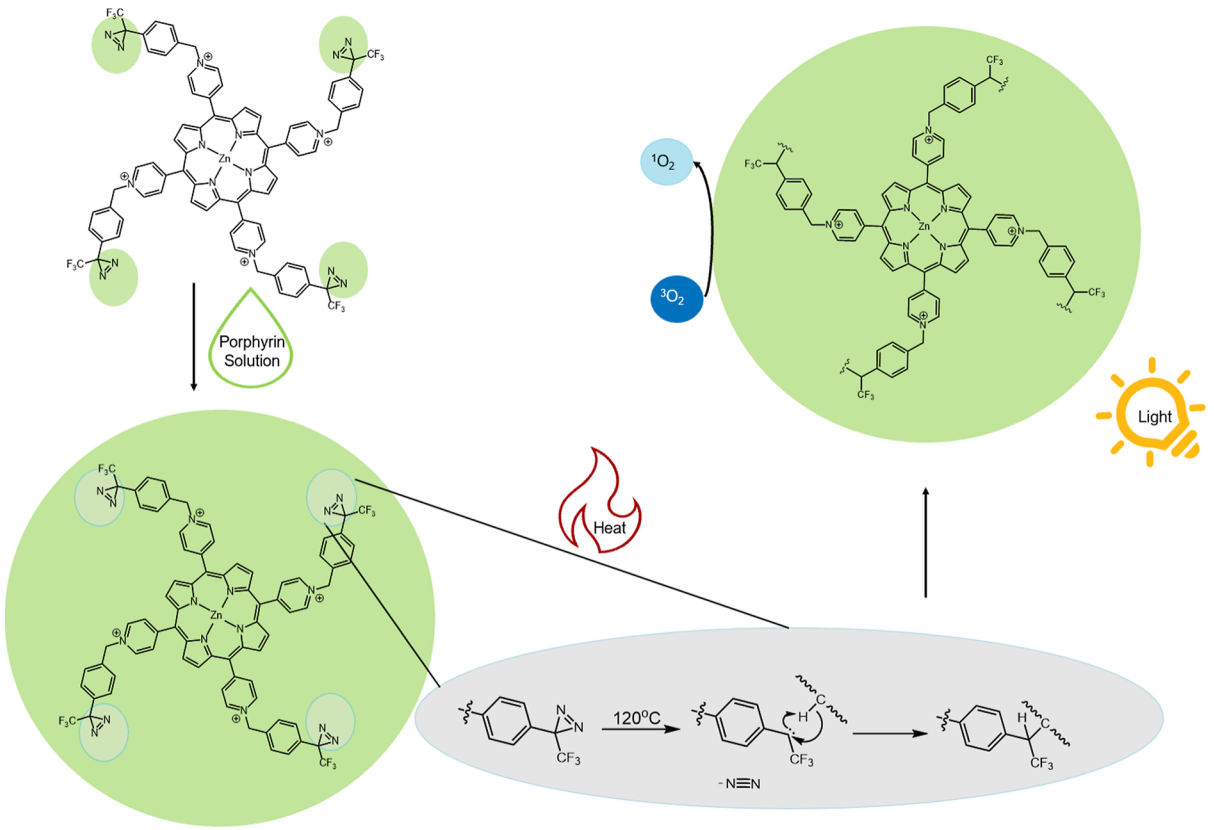

Figure 1. Image illustrating the process of dissolving the porphyrin in solution, followed by coating the molecule on a surface. From there, the diazirine is activated using heat to form the covalent attachment between the molecule and the surface. The material is then activated using visible light to generate singlet oxygen from triplet oxygen.

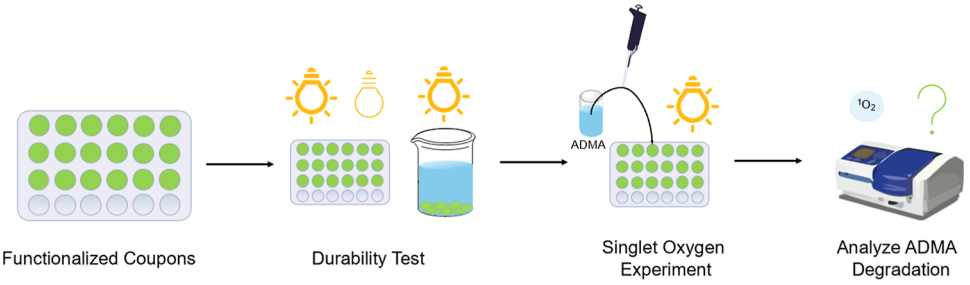

Figure 2. Illustration showing the process of durability against photobleaching tests. Using a set of functionalized coupons, they undergo a durability test of either high intensity light, ambient light, or high intensity light under water. Then, the coupons undergo the singlet oxygen detection experiment before they are analyzed by the ADMA's absorbance to determine singlet oxygen activity.

required to prevent these harmful molecules from entering the environment.

Currently, photodynamic inactivation (PDI) is being investigated as a potential alternative to conventional cleaning agents.[8,19−25] This approach utilizes a photosensitizer, typically an organic molecule, where visible light can activate the molecule to convert triplet oxygen ($^3O_2$) to $^1O_2$.[21,26−31] Previously, we reported an approach of covalently attaching a porphyrin molecule to a polyethylene terephthalate (PET) surface via a heat-activated diazirine moiety for use as an antibacterial material (Figure 1).[32,33] Diazirine chemistry was first utilized to attach small molecules to low surface energy polymers in 2019, through activating the diazirine to form a singlet carbene, which is stabilized by the CF_3 group on the molecule, forming a covalent bond between the molecule and surface.[34,35] The field has expanded to include adhesions of low-surface energy materials and reprocessable thermosets.[35] Due to the porphyrin's ability to mediate $^1O_2$ formation, detected using 9,10-anthrancenediyl-bis-methylene dimalonic acid (ADMA), the material can prevent both planktonic cells and biofilms from growing on the surface.[32,33]

The ability to form a covalent bond between a porphyrin molecule and a polymeric surface postmanufacturing is ideal because an already in-use plastic can still be functionalized to be antimicrobial.[32−34,36]

One major limitation of PDI is inherent in being light-activated: photoactive molecules are also susceptible to photobleaching from too much exposure to light.[37−39] The continuous irradiation of light-sensitive molecules cause chemical changes of the molecular structure over time, preventing absorption of light in the future.[37] This is problematic because the molecule would no longer be able

https://doi.org/10.1021/acsmaterialsau.4c00172
ACS Mater. Au 2025, 5, 537−546

to produce $^1O_2$, thereby causing the material to no longer have antimicrobial properties. Previous studies have shown porphyrinoids that are solid supported or in solid state have better photostability than those in solution.[40,41] Building on this concept, we wanted to further explore how our solid-state porphyrinic material withstands photobleaching by monitoring $^1O_2$ after exposure to various lighting conditions.[42,43] The chosen conditions are photobleaching with a high intensity, ambient light, and underwater (Figure 2). These various conditions were chosen as they are relevant to potential environments the porphyrin-functionalized coupons may be exposed to. Herein, we present the results of the durability of our proof-of-concept light-activated antimicrobial PET.

2. METHODS

2.1. Materials

All chemicals were used as received unless otherwise specified. PET (thickness 0.254 mm) was purchased from McMaster Carr (8567K92). PET was cut into circular coupons (diameter: 15.6 mm). 24-well polystyrene treated cell culture plates were purchased from VWR, USA (10062−896). ADMA (307554−62−7, ≥90%) was purchased from Cayman Chemical Company. Phosphate-buffered solution (PBS) (1x) was purchased from Cytiva (SH30256.02). Methanol (67-56-1, 99%) was purchased from Fischer Scientific (20012043). Luria−Bertani (LB) broth was purchased from Fisher Bioreagents, Canada, and tryptone soya agar (TSA) was purchased from Oxoid, United Kingdom. Sparkleen was purchased from Fisher Scientific (04-320-4). The metal tray used for putting the coupons in the oven to initiate the covalent bond formation was made of aluminum and purchased from Fisher Scientific (13-814-60). Kimwipes (Kimtech) were ordered from Fisher Scientific (06-666A). The light source used was a broad-spectrum white LED light (75 W, 1800 lm, ∼400−700 nm, Satco). A wireless light sensor (701-999, PS-3212) was purchased from PASCO. A microplate vortexer was purchased from VWR (Analog Vortex Mixer). Absorbance measurements were acquired using a Biotek Cytation 5 plate reader.

2.2. Synthesis of Zinc(II) 5,10,15,20-Tetrakis-((*N*-4-[3-(trifluoromethyl)-3*H*-diazirin-3-yl]-benzyl)-4-pyridyl)-21*H*,23*H*-porphine Tetrabromide

The zinc(II) 5,10,15,20-tetrakis((*N*-4-[3-(trifluoromethyl)-3*H*-diazirin-3-yl]benzyl)-4-pyridyl)-21*H*,23*H*-porphine tetrabromide was synthesized as previously reported.[36]

2.3. Coating and Covalent Bonding Procedure

The following procedure was used to coat and covalently bond the diazirine−porphyrin conjugate to PET for all subsequent experiments. Before coating, PET coupons were thoroughly cleaned by sonication for 20 min in a solution of deionized (DI) water with Sparkleen in a large beaker, followed by 20 min of sonication in DI water after thoroughly rinsing Sparkleen away with DI water. The coupons were then rinsed several times with isopropanol and then sonicated for 20 min in isopropanol before being transferred to an amber bottle, which had been cleaned in the same manner and filled with isopropanol.

When it was time to coat the coupons, they were individually removed from the isopropanol solution, then dried with a stream of nitrogen gas, and placed into the wells of a 24-well plate. A porphyrin-methanol solution was made with a concentration of 0.1 mg/400 μL (or an alternative concentration as needed in the optimization of porphyrin loading experiments). To coat the coupons, 400 μL was added into each well. The 24-well plate was then placed on a microplate vortexer at speed 1 for at least an hour, until most of the solvent had evaporated. The plate was then removed from the vortexer and left overnight in a fume hood to allow the remainder of the solvent to evaporate.

The coupons were tipped from the 24-well plate onto an aluminum tray. The tray was placed in an oven at 120 °C for 18 h to induce reaction between diazirine and PET. The coupons were removed from the oven, and any excess unattached porphyrin was removed by rinsing each coupon with methanol and gently drying with a Kimwipe.

2.4. Singlet Oxygen Detection Assay

The singlet oxygen detection assay was performed to detect the presence of $^1O_2$ as follows. Two stock solutions were made, one with PBS and the other with 0.18 mg/mL ADMA in PBS. The light source was set to have a median of ∼35,000 ± 7000 lx across the 24-well plate. At each given time point, a porphyrin-functionalized PET coupon (which had either been exposed to a durability test or not depending on the experiment), 200 μL of PBS, and 200 μL of ADMA solution were added to a well, such that when the entire plate was read at the same time, a range of reaction times was assessed. The time points measured were 4 h, 2 h, 1 h, 30 min, 15 min, and 0 min. After the plate was irradiated, a 200 μL aliquot was transferred from each well that was used in the reaction from the 24-well plate into a 96-well plate to measure the absorbance spectrum of the solution. The spectra were recorded using a Cytation 5 plate reader from 300 to −450 nm, every 1 nm.

2.5. Varying Porphyrin Loading Amounts

The effect on $^1O_2$ production by loading different amounts of porphyrin onto the PET coupons was evaluated. Porphyrin-functionalized PET coupons were made following the coating and covalent bonding procedure, varying the concentration of the porphyrin solution. The following amounts were coated onto coupons in a 24-well plate: 0.4 mg, 0.2 mg, 0.1 mg, 0.042 mg, and 0.016 mg. Once the coupons were coated, covalently bonded, and cleaned with methanol and a Kimwipe, they were tested with a singlet oxygen detection assay. Each porphyrin loading amount was compared by graphing the degradation of ADMA for each condition through using ADMA's maximum absorbance (λ = 379 nm) as a function of time exposed to light and functionalized coupons during the singlet oxygen detection assay. Each loading experiment was performed in triplicate.

2.6. Effect of Varying Light Dose

Porphyrin-functionalized PET coupons were prepared following the coating and covalent bonding procedure. All the functionalized coupons had the same amount of porphyrin on them, chosen from Varying Porphyrin Loading Amounts., 0.1 mg. singlet oxygen detection assay. Each 24-well plate containing three rows of coupons was exposed to a different light intensity. The light intensities were recorded by using the light-meter to measure light intensity at points all over the plate, while noting the highest and lowest values to adjust the lamp so the median values of the range were ∼5000, 15,000, 25000, 35000, and 45,000 lx. Coupons were then tested using the singlet oxygen detection assay. Each light intensity was compared by graphing the degradation of ADMA for each condition through using ADMA's maximum absorbance (λ = 379 nm) as a function of time exposed to light and functionalized coupons during the singlet oxygen detection assay. These experiments were performed in sextuplicate.

2.7. Photobleaching with High Intensity Light

The coupons were prepared following the coating and covalent bonding procedure. The coupons were placed in a 24-well plate and exposed to the same light source that is used for the singlet oxygen detection at a range with a median intensity of ∼35,000 lx for 24 h, 72 h, 1 week, or 2 weeks. After their exposure time had completed, the same coupons were used in a singlet oxygen detection assay, to assess how much the high intensity light exposure impacted their ability to generate $^1O_2$. Each photobleach duration was compared by graphing the degradation of ADMA for each condition through using ADMA's maximum absorbance (λ = 379 nm) as a function of time exposed to light and functionalized coupons during the singlet oxygen detection assay. These experiments were performed in sextuplicate.

2.8. Photobleaching with Ambient Light

The coupons were prepared following the coating and covalent bonding procedure. The coupons were all placed in a 24-well plate

https://doi.org/10.1021/acsmaterialsau.4c00172
ACS Mater. Au 2025, 5, 537−546

and were exposed to the ambient light present in the laboratory, which was ∼450 lx when the light is on (typically 11 h per day). The amount of time they were exposed was 24 h, 72 h, 1 week, and 2 weeks. For the 24 and 72 h exposure time, the lights were left on in the laboratory overnight to ensure maximum exposure for that time period because it is shorter than the other time periods. After their exposure time had completed, the same coupons were used in a singlet oxygen detection assay to assess how much the ambient light exposure influenced their efficiency at generating singlet oxygen. Each photobleaching condition was compared by graphing the degradation of ADMA for each condition through using ADMA's maximum absorbance (λ = 379 nm) as a function of time exposed to light and functionalized coupons during the singlet oxygen detection assay. These experiments were performed as sextuplicate.

2.9. Photobleaching with High Intensity Light under Water

This experiment was designed to be similar to photobleaching with using high intensity light, but instead of dry conditions, the coupons were placed in a beaker of deionized water. The coupons were prepared following the coating and covalent bonding procedure. Subsequently, the coupons were placed in a clean 1 L beaker containing 1 L of deionized water. Using the same light source as previous experiments, the light was shone on the beaker full of the coupons at a median value of ∼35,000 lx. The coupons were exposed to the light in this aqueous environment for 24 and 72 h. After exposure, the coupons were used in a singlet oxygen detection assay. Each photobleach condition was compared by graphing the degradation of ADMA for each condition through using ADMA's maximum absorbance (λ = 379 nm) as a function of time exposed to light and functionalized coupons during the singlet oxygen detection assay. These experiments were performed in sextuplicate.

2.10. Dark under-Water Control

This experiment was designed to be similar to photobleaching with high intensity light under water, but instead, the coupons were underwater and in the dark. The coupons were prepared following the coating and covalent bonding procedure. Subsequently, the coupons were placed in a clean 1 L beaker containing 1 L of deionized water. The coupons were left in the dark in this aqueous environment for 24 and 72 h. After exposure, the coupons were used in a singlet oxygen detection assay. Each photobleach condition was compared by graphing the degradation of ADMA for each condition through using ADMA's maximum absorbance (λ = 379 nm) as a function of time exposed to light and functionalized coupons during the singlet oxygen detection assay. These experiments were performed in sextuplicate.

2.11. Dark Control Experiment

The coupons were prepared and cleaned according to the photobleaching with using high intensity light protocol. Afterward, the coupons were placed in a 24-well plate and wrapped in tin foil. The coupons were left for 96 days. They were then used in a singlet oxygen detection assay. These results are used as a control for how being left in a dry and dark environment for an extended period of time affects the coupons. The control was compared by graphing the degradation of ADMA for each condition through using ADMA's maximum absorbance (λ = 379 nm) as a function of time exposed to light and functionalized coupons during the singlet oxygen detection assay. These experiments were performed in sextuplicate.

2.12. Antimicrobial Activity as a Function of Light Dose

The effect of different irradiance levels on antimicrobial PDI was assessed using broad-spectrum white LED light. The plates were exposed to different illuminance levels: (10,965 ± 195, 6019 ± 287, and 1212 ± 85 lx), which correspond to the following irradiance levels (114.3 ± 1.7, 62.3 ± 2.8, and 12.7 ± 0.8 W/m^2), for 6 h. Both illuminance and irradiance were measured by using a PASCO light sensor.

2.13. Cell Counts

The antimicrobial activity of the photoactive coupons irradiated with different light intensities was assessed against *Escherichia coli* (ATCC 25922), as described previously.[32,33] After overnight incubation of *E. coli* in LB at 37 °C, the bacterial suspension of optical density 600_{nm} = 1 was diluted 1/1000 with LB. Selected wells of 24-well plates were modified by adding photoactive discs that were prepared as described in the coating and covalent bonding procedure. Both modified and unmodified wells were inoculated with 400 μL of a diluted bacterial suspension. Each experiment included a plate that was exposed to different intensities of white LED light as mentioned above, at room temperature (22 °C ± 1) for 6 h. Another 24-well plate, prepared and inoculated as mentioned above, was covered with aluminum foil and incubated in the dark for 6 h. Consequently, each experiment included experimental wells (modified wells containing porphyrin cross-linked coupons exposed to light) and the following control wells: light control (unmodified wells, exposed to light), dark porphyrin control (modified wells, kept in the dark), and dark control (unmodified wells, kept in the dark).

After irradiation, aliquots from each well were serially diluted and plated on TSA. A plate count was performed after overnight incubation at 37 °C. The results were reported as colony-forming unit (CFU)/mL. Each experiment included duplicates for both experimental wells and control wells and was repeated three times. The averages (CFU/mL) obtained from the plate count experiments were used to calculate the average percentage inhibition using the following equation

$$\frac{\text{avg. plate counts of control wells} - \text{avg. plate counts of exptl. wells}}{\text{avg. plate counts of control wells}} \times 100$$

2.14. Statistical Analysis

2.14.1. Singlet Oxygen Assays. All graphs made for the singlet oxygen detection experiments were made using RStudio, and T-Tests were utilized to compare ADMA absorbance values at 4 h to that of the control (unexposed) or in the case of varying porphyrin, loading amount was compared to the largest amount of porphyrin being 0.4 mg. In the case of effect of varying light dose, T-Tests were performed to compare the absorbance values at 4 h to the data set of 45,000 lx (Supporting Information).

2.14.2. Bacterial Assays. Results were presented as mean of CFU/mL ± standard deviation. GRAPHPAD was employed to perform one way ANOVA and T-test ($P < 0.05$).

3. RESULTS AND DISCUSSION

Previously, we demonstrated that zinc(II) 5,10,15,20-tetrakis-((*N*-4-[3-(trifluoromethyl)-3*H*-diazirin-3-yl]benzyl)-4-pyridyl)-21*H*,23*H*-porphine tetrabromide has the ability to covalently bond to PET and be activated with light to generate singlet oxygen, which subsequently killed bacteria.[32,33] Covalent bond formation was supported through control experiments, which indicated that both heat and a porphyrin containing diazirine moieties were required in order for the porphyrin to not rinse away.[32,33] The porphyrin-functionalized PET coupons were previously characterized by their absorbance and fluorescence spectra.[32] Singlet oxygen detection experiments were performed in the aqueous medium PBS due to the solubility of the ADMA and to work in a medium that is commonly used in biological assays.[32,33] Using those results as a starting point, this work expands the scope of knowledge in relation to this molecule and explores how different conditions affect its $^1O_2$ generation and antibacterial properties. To facilitate an expanded range of experiments, an improved, less labor-intensive covalent attachment protocol was used, cutting coating time by 80% to 5 min for 24 coupons. The performance of the functionalized coupons was assessed for different light intensities, different amounts of porphyrin added, and different photobleaching conditions.

The impact of the amount of porphyrin loaded onto each coupon on $^1O_2$ generation was assessed by loading different

https://doi.org/10.1021/acsmaterialsau.4c00172
ACS Mater. Au 2025, 5, 537−546

amounts of porphyrin in the range of 0.016−0.4 mg/coupon. Based on Figure 3, as porphyrin loading on the coupon

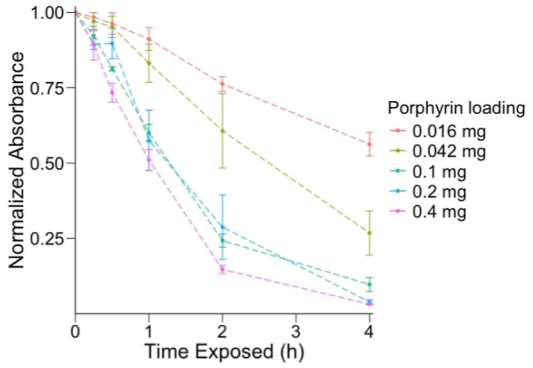

Figure 3. Impact of porphyrin loading on singlet oxygen generation. The maximum absorbance of ADMA (λ = 379 nm) is graphed as a function of time after exposure to 24,000 ± 2000 lx and porphyrin-functionalized PET coupons. Each color represents a different amount of porphyrin loaded onto the coupon. Dashed lines are to show the relationship but do not indicate a continuous data set. Statistical analysis can be found in Supporting Information.

increases, more ADMA is consumed through the reaction with $^1O_2$. Beyond 0.042 mg/coupon, there is no statistical increase in $^1O_2$ production when more porphyrin is loaded; thus, 0.1 mg/coupon was loaded onto each coupon in subsequent experiments to ensure that loadings were well within the range of porphyrin loading to maximize $^1O_2$ generation.

Another factor that impacts singlet oxygen generation, which required investigation, was the effect of varying light intensity. A range of light intensities was assessed in both how they impact cellular growth prevention and $^1O_2$ production. The range of light intensity that was tested was between 5000−45,000 lx, in increments of ∼10,000 lx for $^1O_2$ generation.

The results of this experiment (Figure 4) indicate that the consumption of ADMA increases as the light intensity increases, but the functionalized coupons become saturated with light and reach their maximum potential for $^1O_2$ generation. In a surgical room, an operating table will have

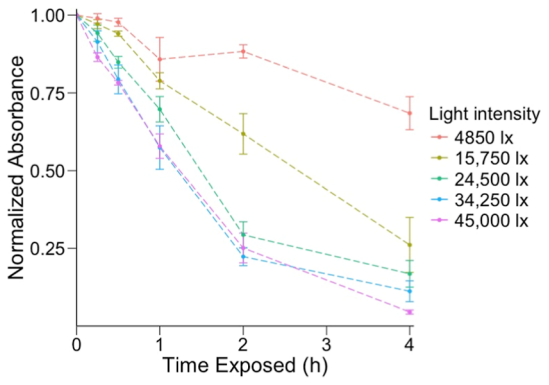

Figure 4. Impact of light intensity on singlet oxygen generation. The maximum absorbance of ADMA (λ = 379 nm) is graphed as a function of time after exposure to light and porphyrin-functionalized PET coupons. Each color represents a different light intensity the functionalized coupons were exposed to in the presence of ADMA. Dashed lines are to show the relationship but do not indicate a continuous data set. Statistical analysis can be found in Supporting Information.

up to 6000 lx at the level of the operating table, so it is beneficial that at this level of light intensity, there is some $^1O_2$ activity.[44] At 15,000 lx, there is no statistical difference in $^1O_2$ generation compared to 45,000 lx, indicating that this is the range where the surface has become saturated with light and has reached its maximum capacity. Based on these results, the subsequent $^1O_2$ detection experiments were performed with ∼35,000 lx and this was chosen as the high light intensity for photobleaching experiments. This was to ensure that the light exposure was above the minimum saturation threshold so the effect would be the same across the 24-well plate.

The antibacterial activity of the functionalized PET discs was assessed quantitatively using plate counts after exposure to different irradiance levels (*a*- 10,965 ± 195, *b*- 6019 ± 287, and *c*- 1212 ± 85 lx). Previously, we had shown our material's ability to prevent planktonic cell and biofilm growth of *Staphylococcus aureus*, *Pseudomonas aeruginosa,* and *E. coli*, whereas in this study, we sought to assess how the amount of light exposure affected the antimicrobial properties.[32,33] The plate count results (CFU/mL) recorded for each condition (light porphyrin, light control, dark porphyrin control, and dark control) after exposure to different irradiance levels are represented in Figure 5a. As determined by one-way ANOVA, the difference in the means of cell counts, recorded for the four conditions exposed to the same irradiance was significant. However, the means of the controls did not demonstrate any significant difference. On the other hand, *t*-test analysis revealed that the means of the light porphyrin plate counts were significantly different when compared with each control separately.

The plate count values were used to calculate percentage inhibition, which represents the average of different "Percentage Inhibition" values calculated with each control. As demonstrated in Figure 5b, the average percentage inhibition was equivalent to 94 ± 2%, 93 ± 2%, and 73 ± 8% after 6 h exposure to irradiance levels equivalent to 10,965 ± 195, 6019 ± 287, and 1212 ± 85 lx, respectively.

Because photobleaching is a potential limitation for long-term applications for light-activated materials, it is important to investigate the porphyrin-functionalized PET's ability to withstand being exposed to light for various amounts of time. The coupons were exposed to the following conditions: high- and low-intensity broadband artificial light as well as high-intensity light underwater. A dark control experiment was also conducted to ensure that the porphyrin was not degrading from open air or underwater.

The high intensity light dose of 35,000 lx was chosen because, as suggested in Figure 4, at this intensity the coupon is saturated with light. Due to the saturation, this is a useful amount of light to expose the coupons for removal and prevention of microbial growth on surfaces; therefore, we wanted to ensure the material could withstand this exposure. The functionalized coupons were pre-exposed to the 35,000 lx for amounts of time between 24 h and 2 weeks. Based on the results (Figure 6), after 24 and 72 h of ∼35,000 lx exposure, the difference in rate of degradation of ADMA is statistically insignificant compared to the unexposed control. This implies that the coupons can withstand photobleaching at this light dose for up to 3 days, which indicates that this amount of light can be used to initiate the coupons' antibacterial properties for up to 3 days without destroying its ability to generate $^1O_2$ in the process. After 1−2 weeks of pre-exposure to the high light intensity, there is a statistically significant decrease of just over

https://doi.org/10.1021/acsmaterialsau.4c00172
ACS Mater. Au 2025, 5, 537−546

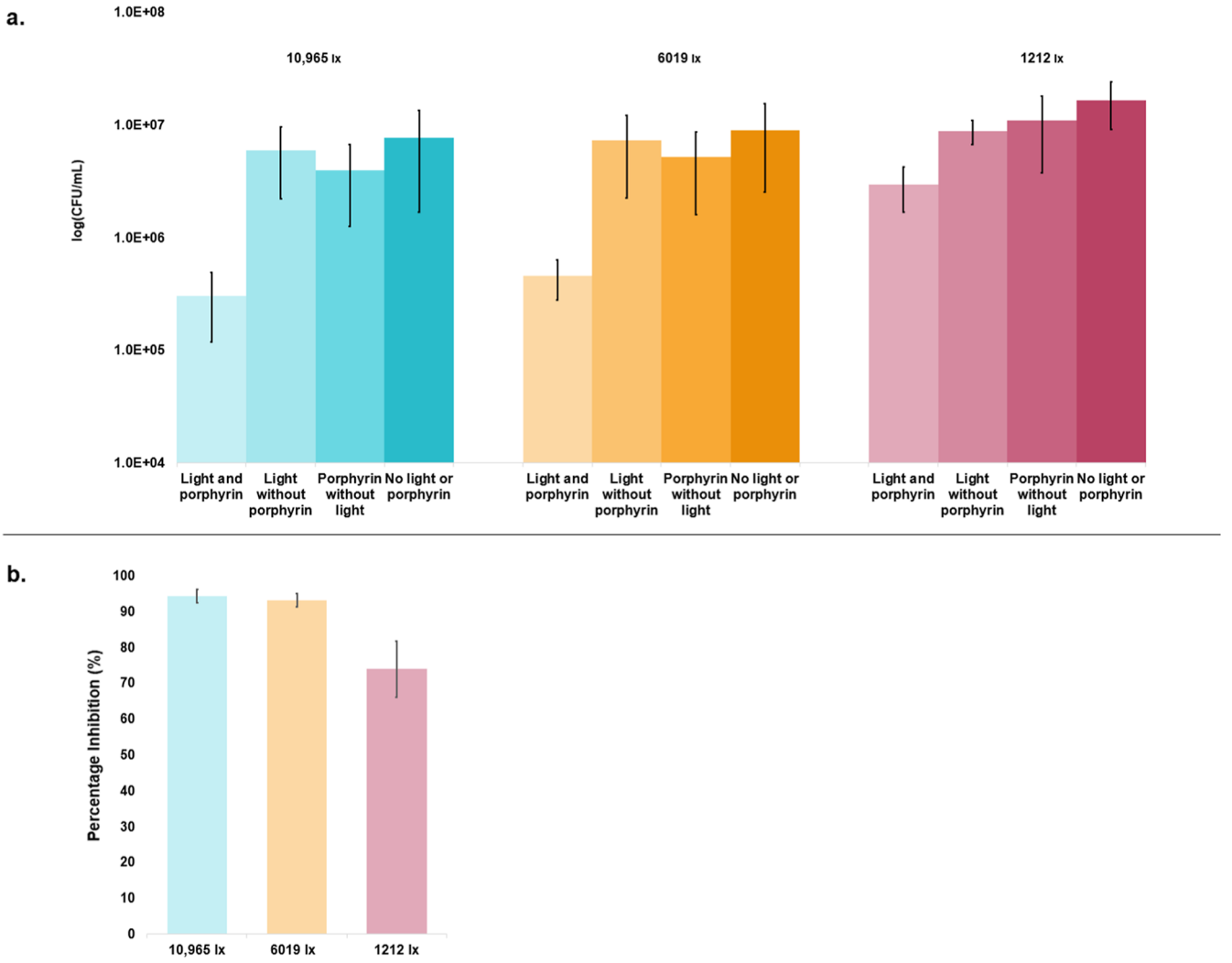

Figure 5. (a) Mean values of *E. coli* cell counts after irradiation with white LED light for 6 h at average irradiance of 10,965 ± 195 lx, 6019 ± 287 lx, and 1212 ± 85 lx ($N = 6$, $P < 0.05$). Statistical analysis information can be found in the Supporting Information. (b) Percentage inhibition of *E. coli* after irradiation with white LED light for 6 h at an average irradiance of 10,965 ± 195 lx, 6019 ± 287 lx, and 1212 ± 85 lx. Statistical analysis information can be found in the Supporting Information.

half compared to the unexposed control. Even with this decrease in $^1O_2$ activity after this duration and intensity of light exposure, there being any $^1O_2$ generation is promising as this is a very high light intensity; operating room tables will have an intensity of up to 6000 lx, while the general lighting in an operating theater can reach up to 4000 lx.[44] Altogether, this further supports the idea that using 35,000 lx to initiate antimicrobial properties of the material is ideal because the functionalized PET is saturated with light and will not be negatively impacted for up to 3 days.

The ambient light dose selected for pre-exposure was 450 lx, which is within the range of typical laboratory or household settings. This was again measured through singlet oxygen detection after the exposure. This would show the ability of the coupons to prevent bacterial growth after sitting under typical ambient conditions for different amounts of time. The pre-exposure times were the same as the high intensity photobleaching experiments, which were 24 h, 72 h, 1 week, and 2 weeks before measuring their singlet oxygen generation through ADMA degradation. The results (Figure 7) indicate that there is no statistical difference between the unexposed control and the data sets for 3 days and 2 weeks, while there are minor statistical differences for the 1 day and 1 week experiments. This is promising for the potential for the material to be used in any setting that has this typical ambient light for longer periods of time since there is no meaningful impact on the $^1O_2$ generation ability.

Previous studies have explored the photostability of porphyrins in solution and for applications in photodynamic therapy (PDT) and in optical devices for bioimaging.[40,45,46] Porphyrins have been determined to have a better photostability when they are coordinated to a metal-center, in this case zinc.[45] Porphyrin photostability has also been investigated through encasing them within a metal−organic framework and complexing them with cyclodextrins for application in PDT.[40,46] In both cases, porphyrin stability was found to have increased compared to the porphyrins remaining not encased or complexed; the photostability was investigated by continuous exposure to light for up to 2 h.[40,46] In both of these cases, the porphyrins were considered highly photostable when retaining their function after 2 h of exposure; our porphyrin-functionalized coupons retain $^1O_2$ production functionality after 2 weeks of exposure of both the ambient and high-

https://doi.org/10.1021/acsmaterialsau.4c00172
ACS Mater. Au 2025, 5, 537−546

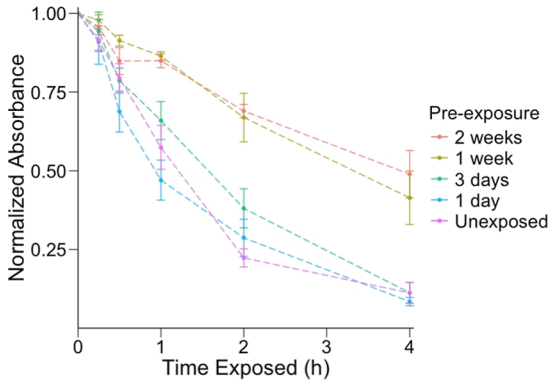

Figure 6. Durability against high intensity (35,000 lx) photobleaching. The maximum absorbance of ADMA (λ = 379 nm) is graphed as a function of time after pre-exposure to 35,000 lx for various durations before being assessed for $^1O_2$ production. Each color represents a different amount of time the functionalized-porphyrin coupons were pre-exposed to 35,000 lx. The unexposed data set is the control that has not been pre-exposed to any light before being tested for singlet oxygen. Dashed lines are to show the relationship but do not indicate a continuous data set. Statistical analysis can be found in Supporting Information.

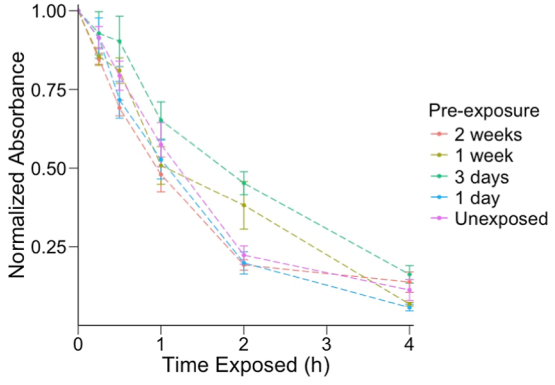

Figure 7. Durability against ambient light (450 lx) photobleaching. The maximum absorbance of ADMA (λ = 379 nm) is graphed as a function of time after pre-exposure to 450 lx for various durations before being assessed for $^1O_2$ production. Each color represents a different amount of time the functionalized-porphyrin coupons were pre-exposed to ambient light (450 lx). The unexposed data set is the control that has not been pre-exposed to any light before being tested for singlet oxygen. Dashed lines are to show the relationship but do not indicate a continuous data set. Statistical analysis can be found in Supporting Information.

intensity light, which compares favorably to these literature examples.[40,46]

We also confirmed that the coupons stop producing $^1O_2$, once the light is turned off by monitoring the degradation of ADMA after exposure to light for 1 h, followed by 1 h of darkness, while still being in the presence of the porphyrin-functionalized coupons (Figure S1).

Another relevant experiment was to explore the effect of high light intensity in aqueous environments. In order to achieve this, the coupons were exposed to over 35,000 lx for 24 or 72 h, while sitting inside of a 1 L beaker containing deionized water (Figure 8). Based on the comparison between the dry and wet conditions, there is a more rapid decline in $^1O_2$ production. Again, there being any $^1O_2$ production under the wet conditions at such a high light intensity shows promise for

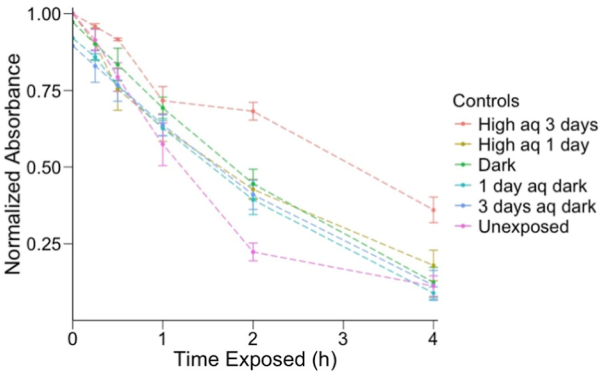

Figure 8. Durability against high intensity photobleaching in water. The maximum absorbance of ADMA (λ = 379 nm) is graphed as a function of time after pre-exposure to 35,000 lx in water for various durations before being assessed for $^1O_2$ production. Each color represents a different condition or control. The dark data sets were the functionalized coupons that were left in the dark for 96 days before being tested. The unexposed data set is the control that has not been pre-exposed to any light before being tested for singlet oxygen. Dashed lines are to show the relationship but do not indicate a continuous data set. Statistical analysis can be found in Supporting Information.

its durability and potential application. Additionally, the water may make the porphyrin more susceptible to photobleaching, which can be seen in literature that various solvents affect the rate of photobleaching by having various effects on stabilizing the intramolecular charge transfer state.[47] When the coupons were left underwater in the dark, there was no statistical difference in $^1O_2$ production, meaning even underwater, light is required to see an impact on $^1O_2$ generation.

As a control experiment, 36 coupons were coated, then covalently bonded with porphyrin, then wrapped in tin foul, and kept in the dark for 96 days. The purpose of this was to ensure that when stored in the absence of light, the porphyrin-coated coupons were not degraded with regard to their $^1O_2$ generating capacity. After the coupons had been left for this time, they were tested for $^1O_2$ generation using ADMA as a singlet oxygen detector (Figure 8). The results indicate that there was no impact on $^1O_2$ production when the coupons were stored in the dark, meaning that light exposure is required to see a decrease in singlet oxygen production. At the same time after 2 weeks of exposure to ambient light, there was also no statistical decrease in $^1O_2$ production, indicating that perhaps ambient light also does not impact the activity of the coupons. Overall, when the coupons are protected from light, they can be stored for long periods of time while maintaining their functionality.

4. CONCLUSIONS

In this work, we explored how both porphyrin loading and different light intensities affect $^1O_2$ generation for a porphyrin-functionalized PET surface, while exploring the capacity of the porphyrin-functionalized material to withstand photobleaching under high-intensity and ambient light conditions. The functionalized PET coupons were assessed on their ability to generate $^1O_2$ after various photobleaching conditions through a singlet oxygen detection assay using ADMA as a detector molecule. The photobleaching conditions that were assessed were a high intensity (35,000 lx), high intensity (35,000 lx) in water, and ambient light (450 lx). It was determined that when

https://doi.org/10.1021/acsmaterialsau.4c00172
ACS Mater. Au 2025, 5, 537−546

photobleached by ∼35,000 lx, the same light intensity for optimal $^1O_2$ generation, the coupons still generate $^1O_2$ even after 2 weeks of exposure. At ∼35,000 lx underwater, there is a greater impact on the ability to generate $^1O_2$ than that under dry conditions, but there is still activity, which is again promising for such a high light intensity. Under ambient light around 450 lx, there is no statistical impact on the coupons ability to generate singlet oxygen. When stored in the absence of light, the coupons are as effective at $^1O_2$ generation as they would be if immediately tested when stored for at least 96 days. These results indicate that the material has potential to remain useful for an extended period if left under ambient light and an even longer time if protected from light.

The following files are available free of charge.

■ ASSOCIATED CONTENT

Supporting Information

The Supporting Information is available free of charge at https://pubs.acs.org/doi/10.1021/acsmaterialsau.4c00172.

Statistical analysis for results of each experiment and additional data for ADMA degradation in the dark after light exposure (PDF)

■ AUTHOR INFORMATION

Corresponding Author

Heather L. Buckley − *Department of Chemistry, University of Victoria, Victoria, British Columbia V8P 5C2, Canada; Department of Civil Engineering, Centre for Advanced Materials and Related Technologies (CAMTEC), and Institute for Integrated Energy Systems (IESVic), University of Victoria, Victoria, British Columbia V8P 5C2, Canada;* orcid.org/0000-0001-7147-0980; Email: hbuckley@uvic.ca

Authors

Grace M.O. Tieman − *Department of Chemistry, University of Victoria, Victoria, British Columbia V8P 5C2, Canada; Centre for Advanced Materials and Related Technologies (CAMTEC) and Institute for Integrated Energy Systems (IESVic), University of Victoria, Victoria, British Columbia V8P 5C2, Canada*

Fatima Shatila − *Department of Civil Engineering, Centre for Advanced Materials and Related Technologies (CAMTEC), and Institute for Integrated Energy Systems (IESVic), University of Victoria, Victoria, British Columbia V8P 5C2, Canada*

Stefania Ceschia − *Department of Civil Engineering, University of Victoria, Victoria, British Columbia V8P 5C2, Canada*

Jeremy E. Wulff − *Department of Chemistry, University of Victoria, Victoria, British Columbia V8P 5C2, Canada; Centre for Advanced Materials and Related Technologies (CAMTEC), University of Victoria, Victoria, British Columbia V8P 5C2, Canada;* orcid.org/0000-0001-9670-160X

Complete contact information is available at: https://pubs.acs.org/10.1021/acsmaterialsau.4c00172

Author Contributions

G.T. wrote the manuscript with help from F.S. writing the microbiology sections. G.T. designed and performed the updated covalent bonding procedure, the assessments of varying light intensities and porphyrin amounts, and the durability experiments. F.S. designed and performed the microbiology experiments. S.C. graphed and performed statistical analysis of the varying porphyrin amounts, varying light intensities, and durability experiments. J.W. provided mentorship on experimental design, data analysis, and editorial feedback on the manuscript. H.B. acquired funding to support the project and provided mentorship on experimental design and editorial feedback on the manuscript. All authors have given approval to the final version of the manuscript.

Funding

We gratefully acknowledge Mitacs Canada (grant IT17318) and our industry partners, Epic Ventures, for fellowships and consumables support to G.T., F.S., and S.C. We also are grateful for support from the IESVic Clean Energy Systems Accelerator Program (IESVic-CESAP) IRAP, NSERC USRA.

Notes

The authors declare the following competing financial interest(s): Authors Buckley and Wulff are co-authors on a patent (WO/2021/179064) that claims the use of the zinc(II) porphine described in this work as light-activated pathogen-killing molecule. There are no additional conflicts.

■ ACKNOWLEDGMENTS

The authors thank Rebecca Hof for training and support. Figures (2 and TOC) were created using ChemDraw version 23.

■ ABBREVIATIONS

PDI, photodynamic inactivation; 1O2, singlet oxygen; ROS, reactive oxygen species; PET, polyethylene terephthalate; HAI, hospital-acquired infection; CBD, chlorine-based disinfectant; DBP, disinfection byproduct; 3O2, triplet oxygen; ADMA, 9,10-anthrancenediyl-bis-methylene dimalonic acid; CFU, colony-forming unit; OD, optical density; MOF, metal−organic framework

■ REFERENCES

(1) Peleg, A. Y.; Hooper, D. C. Hospital-Acquired Infections Due to Gram-Negative Bacteria. *N. Engl. J. Med.* **2010**, *362*, 1804−1817.

(2) Mahira, S.; Jain, A.; Khan, W.; Domb, A. J. Chapter 1. Antimicrobial Materials—An Overview. In *Antimicrobial Materials for Biomedical Applications*; The Royal Society of Chemistry, 2019; pp 1−37..

(3) Hashempour-Baltork, F.; Hosseini, H.; Shojaee-Aliabadi, S.; Torbati, M.; Alizadeh, A. M.; Alizadeh, M. Drug Resistance and the Prevention Strategies in Food Borne Bacteria: An Update Review. *Adv. Pharm. Bull.* **2019**, *9* (3), 335−347.

(4) Jin, M.; Liu, L.; Wang, D.-n.; Yang, D.; Liu, W.-l.; Yin, J.; Yang, Z.-w.; Wang, H.; Qiu, Z.-g.; Shen, Z.-q.; Shi, D.-y.; Li, H.-b.; Guo, J.-h.; Li, J. w. Chlorine Disinfection Promotes the Exchange of Antibiotic Resistance Genes across Bacterial Genera by Natural Transformation. *ISME J.* **2020**, *14* (7), 1847−1856.

(5) Akarsu, E.; Uslu, R. Light-Activated Hybrid Organic/Inorganic Antimicrobial Coatings. *J. Sol-Gel Sci. Technol.* **2018**, *87* (1), 183−194.

(6) Abban, M. K.; Ayerakwa, E. A.; Mosi, L.; Isawumi, A. The Burden of Hospital Acquired Infections and Antimicrobial Resistance. *Heliyon* **2023**, *9* (10), No. e20561.

(7) Shineh, G.; Mobaraki, M.; Perves Bappy, M. J.; Mills, D. K. Biofilm Formation, and Related Impacts on Healthcare, Food Processing and Packaging, Industrial Manufacturing, Marine Indus-

tries, and Sanitation−A Review. *Appl. Microbiol.* **2023**, *3* (3), 629−665.
(8) Koshani, R.; Zhang, J.; Van De Ven, T. G. M.; Lu, X.; Wang, Y. Modified Hairy Nanocrystalline Cellulose as Photobactericidal Nanofillers for Food Packaging Application. *ACS Sustain. Chem. Eng.* **2021**, *9* (31), 10513−10523.
(9) Da-Silva-Correa, L. H.; Smith, H.; Thibodeau, M. C.; Welsh, B.; Buckley, H. L. The Application of Non-Oxidizing Biocides to Prevent Biofouling in Reverse Osmosis Polyamide Membrane Systems: A Review. *J. Water Supply:Res. Technol.–AQUA* **2022**, *71* (2), 261−292.
(10) Luo, X.; Zhang, B.; Lu, Y.; Mei, Y.; Shen, L. Advances in Application of Ultraviolet Irradiation for Biofilm Control in Water and Wastewater Infrastructure. *J. Hazard. Mater.* **2022**, *421*, 126682.
(11) Parveen, N.; Chowdhury, S.; Goel, S. Environmental Impacts of the Widespread Use of Chlorine-Based Disinfectants during the COVID-19 Pandemic. *Environ. Sci. Pollut. Res.* **2022**, *29* (57), 85742−85760.
(12) Ankit; Kumar, A.; Jain, V.; Deovanshi, A.; Lepcha, A.; Das, C.; Bauddh, K.; Srivastava, S. Environmental Impact of COVID-19 Pandemic: More Negatives than Positives. *Environ. Sustainability* **2021**, *4* (3), 447−454.
(13) Li, X. F.; Mitch, W. A. Drinking Water Disinfection Byproducts (DBPs) and Human Health Effects: Multidisciplinary Challenges and Opportunities. *Environ. Sci. Technol.* **2018**, *52* (4), 1681−1689.
(14) Gray, M. J.; Wholey, W.-Y.; Jakob, U. Bacterial Responses to Reactive Chlorine Species. *Annu. Rev. Microbiol.* **2013**, *67* (1), 141−160.
(15) Kalita, I.; Kamilaris, A.; Havinga, P.; Reva, I. Assessing the Health Impact of Disinfection Byproducts in Drinking Water. *ACS ES&T Water* **2024**, *4* (4), 1564−1578.
(16) Srivastav, A. L.; Patel, N.; Chaudhary, V. K. Disinfection By-Products in Drinking Water: Occurrence, Toxicity and Abatement. *Environ. Pollut.* **2020**, *267*, 115474.
(17) Saiz-Lopez, A.; Von Glasow, R. Reactive Halogen Chemistry in the Troposphere. *Chem. Soc. Rev.* **2012**, *41* (19), 6448.
(18) Chu, W.; Fang, C.; Deng, Y.; Xu, Z. Intensified Disinfection Amid COVID-19 Pandemic Poses Potential Risks to Water Quality and Safety. *Environ. Sci. Technol.* **2021**, *55* (7), 4084−4086.
(19) Valkov, A.; Nakonechny, F.; Nisnevitch, M. Polymer-Immobilized Photosensitizers for Continuous Eradication of Bacteria. *Int. J. Mol. Sci.* **2014**, *15* (9), 14984−14996.
(20) Nakonechny, F.; Barel, M.; David, A.; Koretz, S.; Litvak, B.; Ragozin, E.; Etinger, A.; Livne, O.; Pinhasi, Y.; Gellerman, G.; Nisnevitch, M. Dark Antibacterial Activity of Rose Bengal. *Int. J. Mol. Sci.* **2019**, *20*, 3196.
(21) Pereira, M. A.; Faustino, M. A. F.; Tomé, J. P. C.; Neves, M. G. P. M. S.; Tomé, A. C.; Cavaleiro, J. A. S.; Cunha, A.ˆ.; Almeida, A. Influence of External Bacterial Structures on the Efficiency of Photodynamic Inactivation by a Cationic Porphyrin. *Photochem. Photobiol. Sci.* **2014**, *13* (4), 680−690.
(22) Wright, T.; Vlok, M.; Shapira, T.; Olmstead, A. D.; Jean, F.; Wolf, M. O. Photodynamic and Contact Killing Polymeric Fabric Coating for Bacteria and SARS-CoV-2. *ACS Appl. Mater. Interfaces* **2022**, *14* (1), 49−56.
(23) Zeng, Y.; Wolf, M. O. Antimicrobial Textiles Based on Photocrosslinked Poly(Ethylene- *Co* -Acrylic Acid). *RSC Appl. Polym.* **2024**, *2*, 1057−1061.
(24) Kirar, S.; Reddy, Y. N.; Chand Banerjee, U.; Bhaumik, J. Development of Meso-Substituted Heterocyclic BODIPY-Based Polymeric Nanoparticles for Pathogen Inhibition using Photodynamic Therapy**. *ChemPhotoChem* **2023**, *7*, No. e202200172.
(25) Macia, N.; Bresoli-Obach, R.; Nonell, S.; Heyne, B. Hybrid Silver Nanocubes for Improved Plasmon-Enhanced Singlet Oxygen Production and Inactivation of Bacteria. *J. Am. Chem. Soc.* **2019**, *141* (1), 684−692.
(26) Peddinti, B. S. T.; Scholle, F.; Ghiladi, R. A.; Spontak, R. J. Photodynamic Polymers as Comprehensive Anti-Infective Materials: Staying Ahead of a Growing Global Threat. *ACS Appl. Mater. Interfaces* **2018**, *10* (31), 25955−25959.
(27) Peddinti, B. S. T.; Morales-Gagnon, N.; Pourdeyhimi, B.; Scholle, F.; Spontak, R. J.; Ghiladi, R. A. Photodynamic Coatings on Polymer Microfibers for Pathogen Inactivation: Effects of Application Method and Composition. *ACS Appl. Mater. Interfaces* **2021**, *13*, 155−163.
(28) Larsen, S.; Adewuyi, J. A.; Ung, G.; Ghosh, A. Transition-Metal Isocorroles as Singlet Oxygen Sensitizers. *Inorg. Chem.* **2023**, *62* (19), 7483−7490.
(29) Sahu, K.; Angeloni, S.; Conradie, J.; Villa, M.; Nayak, M.; Ghosh, A.; Ceroni, P.; Kar, S. NIR-Emissive, Singlet-Oxygen-Sensitizing Gold Tetra(Thiocyano)Corroles. *Dalton Trans.* **2022**, *51* (35), 13236−13245.
(30) Reddy, Y. N.; Kirar, S.; Thakur, N. S.; Patil, M. D.; Bhaumik, J. Sunlight Assisted Photocatalytic Valorization of Lignin Using Recyclable Light Harvesters. *ACS Sustain. Chem. Eng.* **2023**, *11* (12), 4568−4579.
(31) Macia, N.; Kabanov, V.; Heyne, B. Rationalizing the Plasmonic Contributions to the Enhancement of Singlet Oxygen Production. *J. Phys. Chem. C* **2020**, *124* (6), 3768−3777.
(32) Musolino, S. F.; Shatila, F.; Tieman, G. M. O.; Masarsky, A. C.; Thibodeau, M. C.; Wulff, J. E.; Buckley, H. L. Light-Induced Anti-Bacterial Effect Against Staphylococcus Aureus of Porphyrin Covalently Bonded to a Polyethylene Terephthalate Surface. *ACS Omega* **2022**, *7* (33), 29517−29525.
(33) Shatila, F.; Tieman, G. M. O.; Musolino, S. F.; Wulff, J. E.; Buckley, H. L. Antimicrobial Photodynamic Inactivation of Planktonic and Biofilm Cells by Covalently Immobilized Porphyrin on Polyethylene Terephthalate Surface. *Int. Biodeterior. Biodegrad.* **2023**, *178*, 105567.
(34) Lepage, M. L.; Simhadri, C.; Liu, C.; Takaffoli, M.; Bi, L.; Crawford, B.; Milani, A. S.; Wulff, J. E. A Broadly Applicable Cross-Linker for Aliphatic Polymers Containing C-H Bonds. *Science* **2019**, *366*, 875−878.
(35) Lepage, M. L.; Musolino, S. F.; Wulff, J. E. Design, Exploitation, and Rational Improvements of Diazirine-Based Universal Polymer Crosslinkers. *Acc. Chem. Res.* **2024**, *57* (22), 3327−3342.
(36) Cuthbert, T. J.; Ennis, S.; Musolino, S. F.; Buckley, H. L.; Niikura, M.; Wulff, J. E.; Menon, C. Covalent Functionalization of Polypropylene Filters with Diazirine−Photosensitizer Conjugates Producing Visible Light Driven Virus Inactivating Materials. *Sci. Rep.* **2021**, *11*, 19029.
(37) Bonnett, R.; Martínez, G. Photobleaching of Sensitisers Used in Photodynamic Therapy. *Tetrahedron* **2001**, *57* (47), 9513−9547.
(38) Tasso, T. T.; Schlothauer, J. C.; Junqueira, H. C.; Matias, T. A.; Araki, K.; Liandra-Salvador, E.ˆ.; Antonio, F. C. T.; Homem-de-Mello, P.; Baptista, M. S. Photobleaching Efficiency Parallels the Enhancement of Membrane Damage for Porphyrazine Photosensitizers. *J. Am. Chem. Soc.* **2019**, *141* (39), 15547−15556.
(39) Bonnett, R.; Djelal, B. D.; Hamilton, P. A.; Martinez, G.; Wierrani, F. Photobleaching of 5,10,15,20-Tetrakis(m-Hydroxyphenyl)Porphyrin (m-THPP) and the Corresponding Chlorin (m-THPC) and Bacteriochlorin(m-THPBC). A Comparative Study. *J. Photochem. Photobiol., B* **1999**, *53* (1−3), 136−143.
(40) Hassan, G. F.; El Hoda Saad, N.; Hmadeh, M.; Karam, P. Enhancing Porphyrin Photostability When Locked in Metal−Organic Frameworks. *Dalton Trans.* **2018**, *47* (44), 15765−15771.
(41) Gamelas, S. R. D.; Tomé, J. P. C.; Tomé, A. C.; Lourenço, L. M. O. Porphyrin-Containing Materials for Photodegradation of Organic Pollutants in Wastewaters: A Review. *Catal. Sci. Technol.* **2024**, *14* (9), 2352−2389.
(42) Felgenträger, A.; Maisch, T.; Späth, A.; Schröder, J. A.; Bäumler, W. Singlet Oxygen Generation in Porphyrin-Doped Polymeric Surface Coating Enables Antimicrobial Effects on Staphylococcus Aureus. *Phys. Chem. Chem. Phys.* **2014**, *16* (38), 20598−20607.
(43) Jiang, H.; Guo, G.; Chen, W.; Cui, Z. Reactive Dyeing of Synthetic Fibers Employing Dyes Containing a Diazirine Moiety. *Dyes Pigm.* **2021**, *194*, 109555.

https://doi.org/10.1021/acsmaterialsau.4c00172
ACS Mater. Au 2025, 5, 537−546

(44) Hemphälä, H.; Osterhaus, W.; Larsson, P.; Borell, J.; Nylén, P. Towards Better Lighting Recommendations for Open Surgery. *Light. Res. Technol.* **2020**, *52* (7), 856−882.
(45) Golec, B.; Buczyńska, J.; Nawara, K.; Gorski, A.; Waluk, J. Photodegradation of Free Base and Zinc Porphyrins in the Presence and Absence of Oxygen. *Photochem. Photobiol. Sci.* **2023**, *22* (12), 2725−2734.
(46) Ohishi, Y.; Ichikawa, T.; Yokoyama, S.; Yamashita, J.; Iwamura, M.; Nozaki, K.; Zhou, Y.; Chiba, J.; Inouye, M. Water-Soluble Rotaxane-Type Porphyrin Dyes as a Highly Membrane-Permeable and Durable Photosensitizer Suitable for Photodynamic Therapy. *ACS Appl. Bio Mater.* **2024**, *7* (10), 6656−6664.
(47) Woodford, O.; Harriman, A.; McFarlane, W.; Wills, C. Dramatic Effect of Solvent on the Rate of Photobleaching of Organic Pyrrole-BF2 (BOPHY) Dyes. *ChemPhotoChem* **2017**, *1*, 317−325.

https://doi.org/10.1021/acsmaterialsau.4c00172
ACS Mater. Au 2025, 5, 537−546